



# 2020「中技社科技獎學金」

2020 CTCI Foundation Science and Technology Scholarship

## 境外生研究獎學金

Research Scholarship for International Graduate Students



### 鈷鉑合金在二維材料上的磁性特性

### Magnetism of CoPd on two-dimension material

國立臺灣師範大學 物理系

博士班一年級 廖澤銘 (edward2010619@gmail.com) 指導教授：林文欽 博士 (wclin@ntnu.edu.tw)

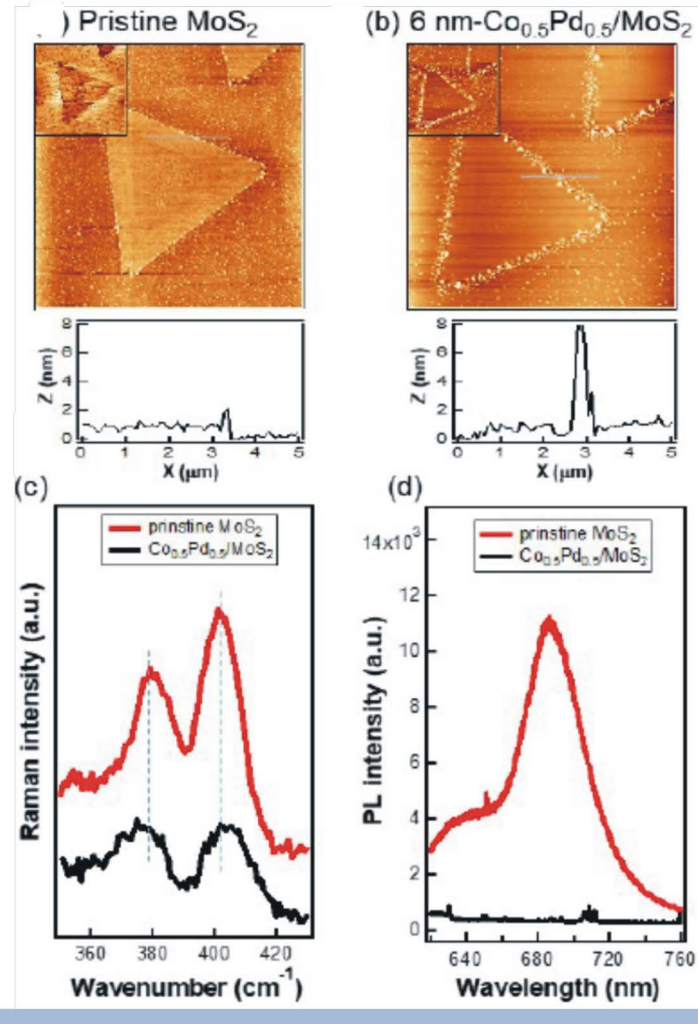
#### 研究重點

First part, CoPd alloy nanostructures and thin films were deposited on MoS<sub>2</sub> flakes through e-beam evaporation at a high temperature (HT) (500 K) and at room temperature (RT) (300 K). In HT growth, CoPd nanoparticles assembled at the edge of the MoS<sub>2</sub> flake. As indicated by the quenched photoluminescence, HT deposition resulted in a flat CoPd coverage with a roughness of  $\pm 0.5$  nm on a MoS<sub>2</sub> terrace. By contrast, RT growth led to a relatively rough CoPd thin film on MoS<sub>2</sub> (roughness  $\pm 2$  nm). The film comprised a merged nanoparticle assembly. The MoS<sub>2</sub>/SiO<sub>2</sub> step edge played a crucial role in magnetic domain pinning such that the magnetic coercivity (H<sub>c</sub>) of Pd/Co/MoS<sub>2</sub> was smaller than that of Pd/Co/SiO<sub>2</sub>. Similarly, RT CoPd (8 nm)/MoS<sub>2</sub> exhibited a parallelogram-shaped hysteresis loop with a relatively small H<sub>c</sub> value compared with that of the square hysteresis loops of RT CoPd (8 nm)/SiO<sub>2</sub>. Second part, we propose a new method to fabricate micro-structured magnetic domains using patterned single-layer Gr. In the first experiment, single-layer Gr was transferred onto a CoPd alloy film pre-grown on a SiO<sub>2</sub>/Si(001) substrate. Subsequently, the single-layer Gr was patterned through electron beam lithography followed by oxygen plasma etching to expose selective micron-sized areas of CoPd. The exposed areas of CoPd were more easily oxidized compared to the areas protected by Gr. In the second experiment, a lithographically-patterned Gr layer was placed between the Fe and CoPd films to block interlayer diffusion area-selectively during sample annealing, and magnetic contrast was observed to be established between the Pd/Fe/Gr/CoPd and Pd/Fe/CoPd areas, leading to a magnetic structure that matched the Gr patterning. These observations demonstrate that Gr patterning is a simple and powerful method of fabricating spintronic devices.

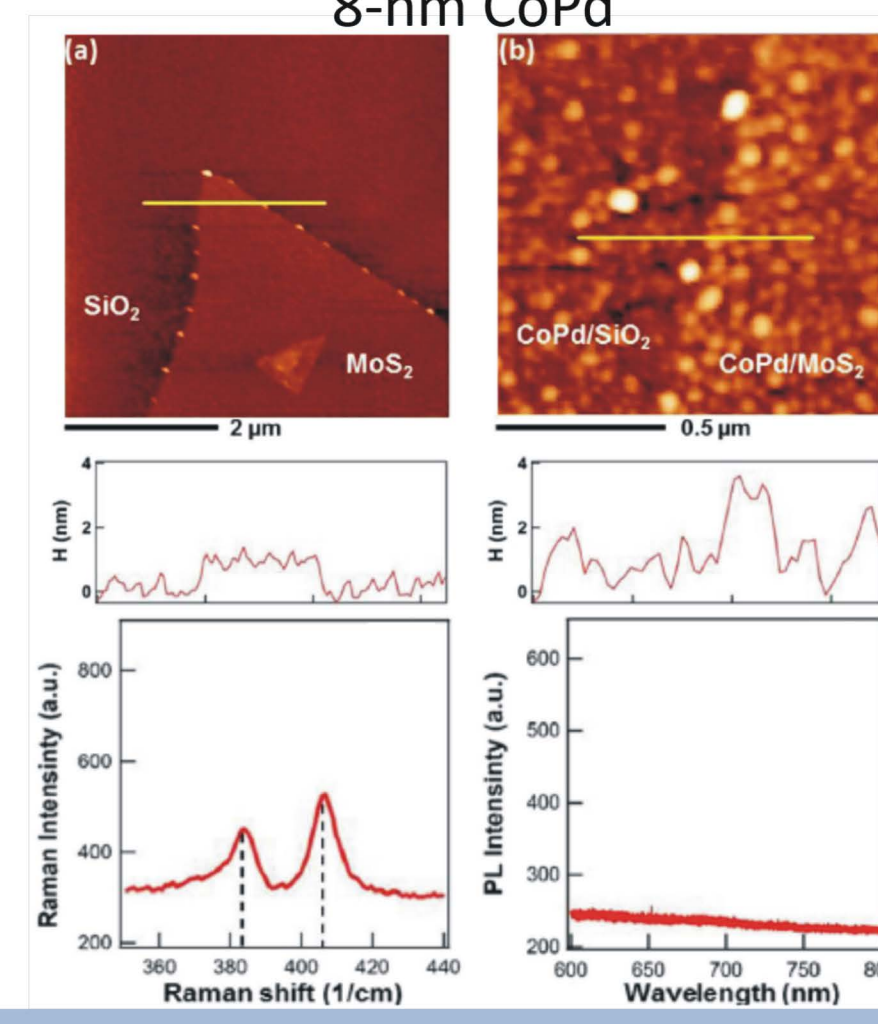
#### 研究結果

##### Morphology of room-temperature(RT) deposition and high-temperature(HT) deposition CoPd/MoS<sub>2</sub>

###### (a) Characterization of HT -deposited 6-nm CoPd



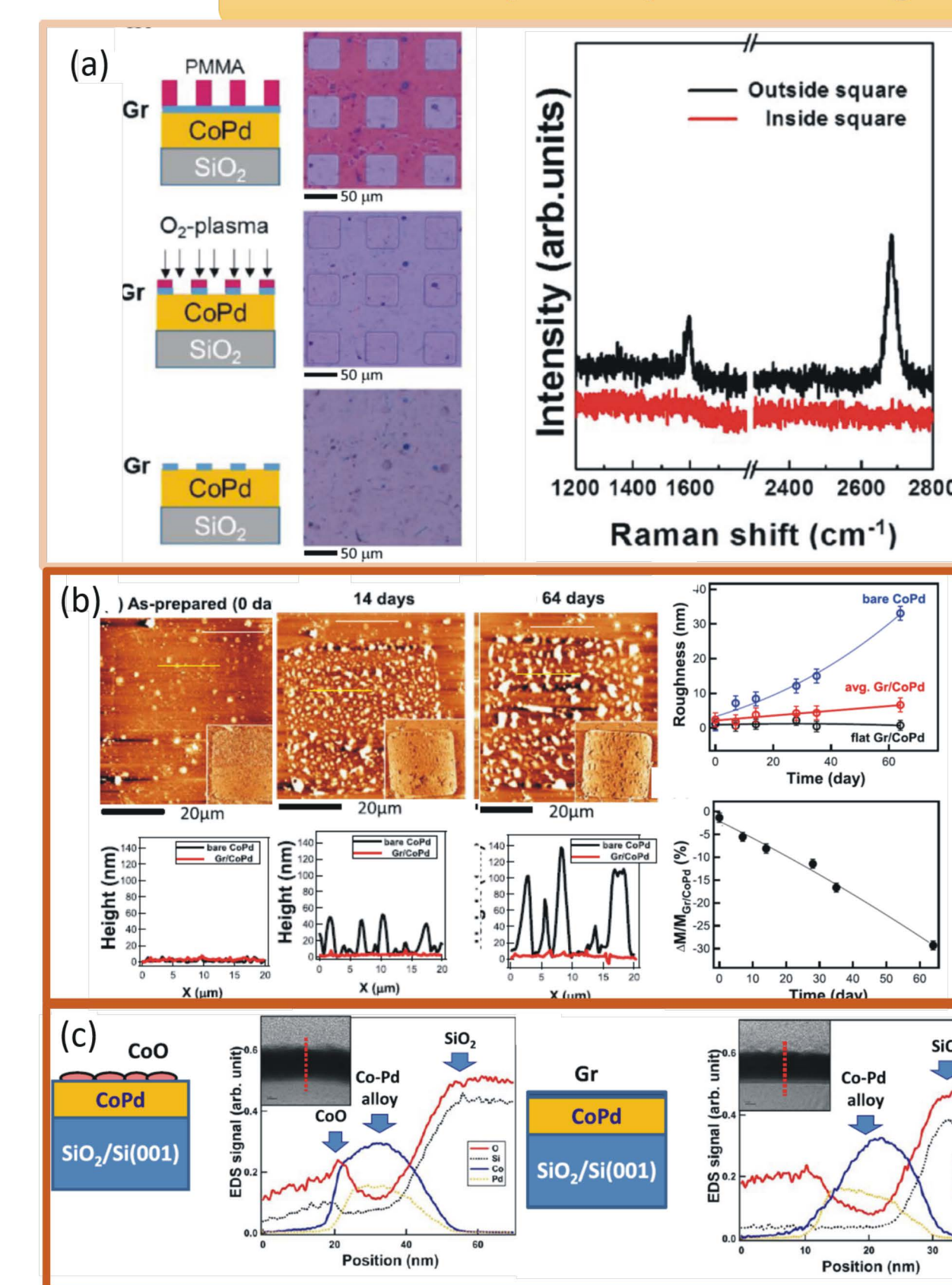
###### (b) Characterization of RT -deposited 8-nm CoPd



(a) The HT deposition of CoPd on the MoS<sub>2</sub> surface resulted in a uniform coverage with a roughness less than 1nm. The cluster nucleation at the MoS<sub>2</sub> edge as previously reported, the topography on the MoS<sub>2</sub> terrace remained at and the roughness was within 1 nm.

(b) After deposition of 8-nm Co-Pd at RT, the MoS<sub>2</sub>-SiO<sub>2</sub> step became indistinct and the MoS<sub>2</sub> surface comprised CoPd nanoparticles with a size of approximately tens of nano-meters. because the surface energy of the deposit is higher than that of the substrate, and the interaction between the deposit and substrate is weak.

##### Graphene protection against oxidation



(a) The single-layer Gr was patterned through electron beam lithography followed by oxygen plasma etching to expose selective micron-sized areas of CoPd.

(b) shows the change in the surface morphology of the patterned-Gr/CoPd sample under ambient conditions for 0–64 day after fabrication. Also Evolution of the difference in the Kerr intensity between the bare CoPd and Gr/CoPd areas normalized by the Kerr intensity of Gr/CoPd as a function of the ambient exposure time.

(c) TEM cross-sectional EDS depth profiles and elemental mapping for (a) bare CoPd and (b) Gr/CoPd areas.

##### Magnetism of room-temperature(RT) deposition and high-temperature(HT) deposition CoPd/MoS<sub>2</sub>

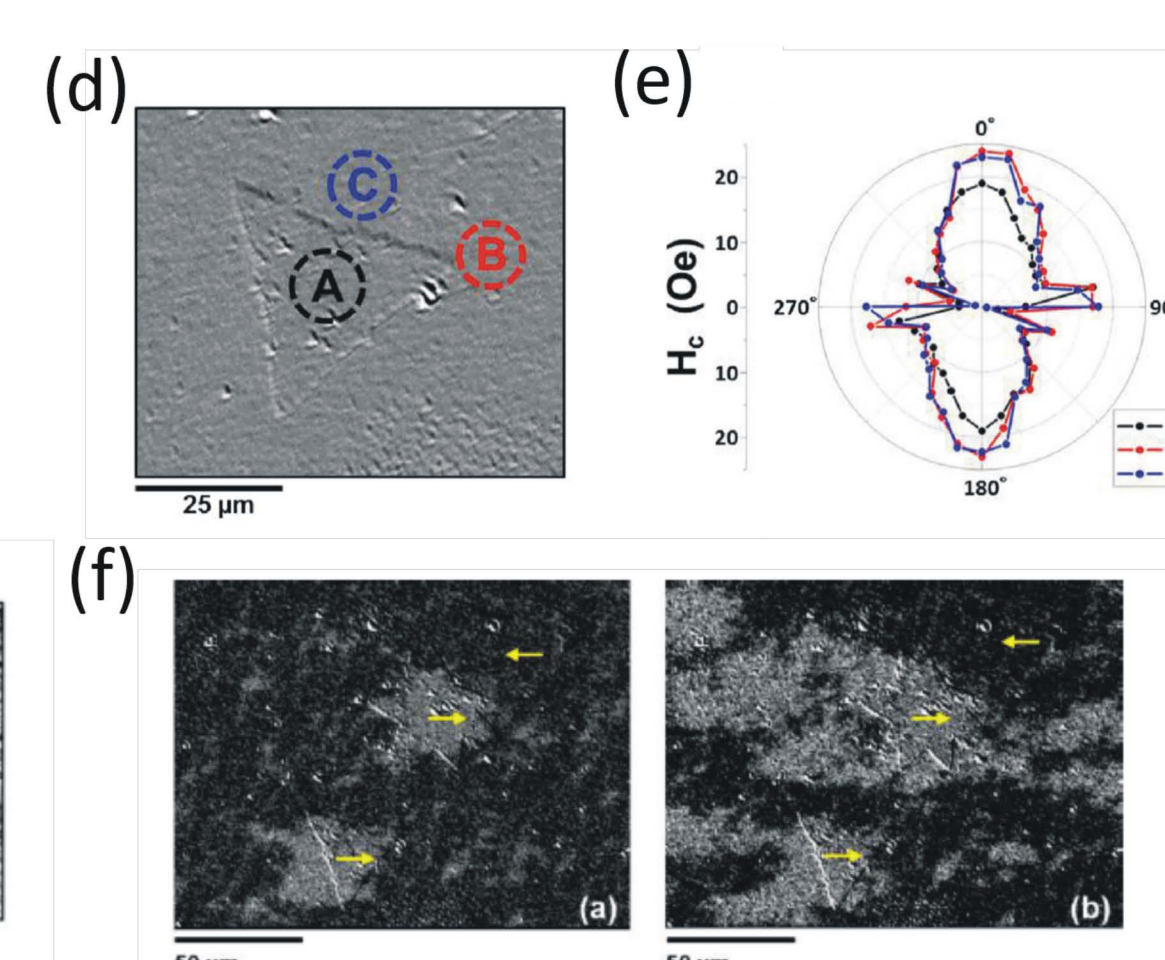
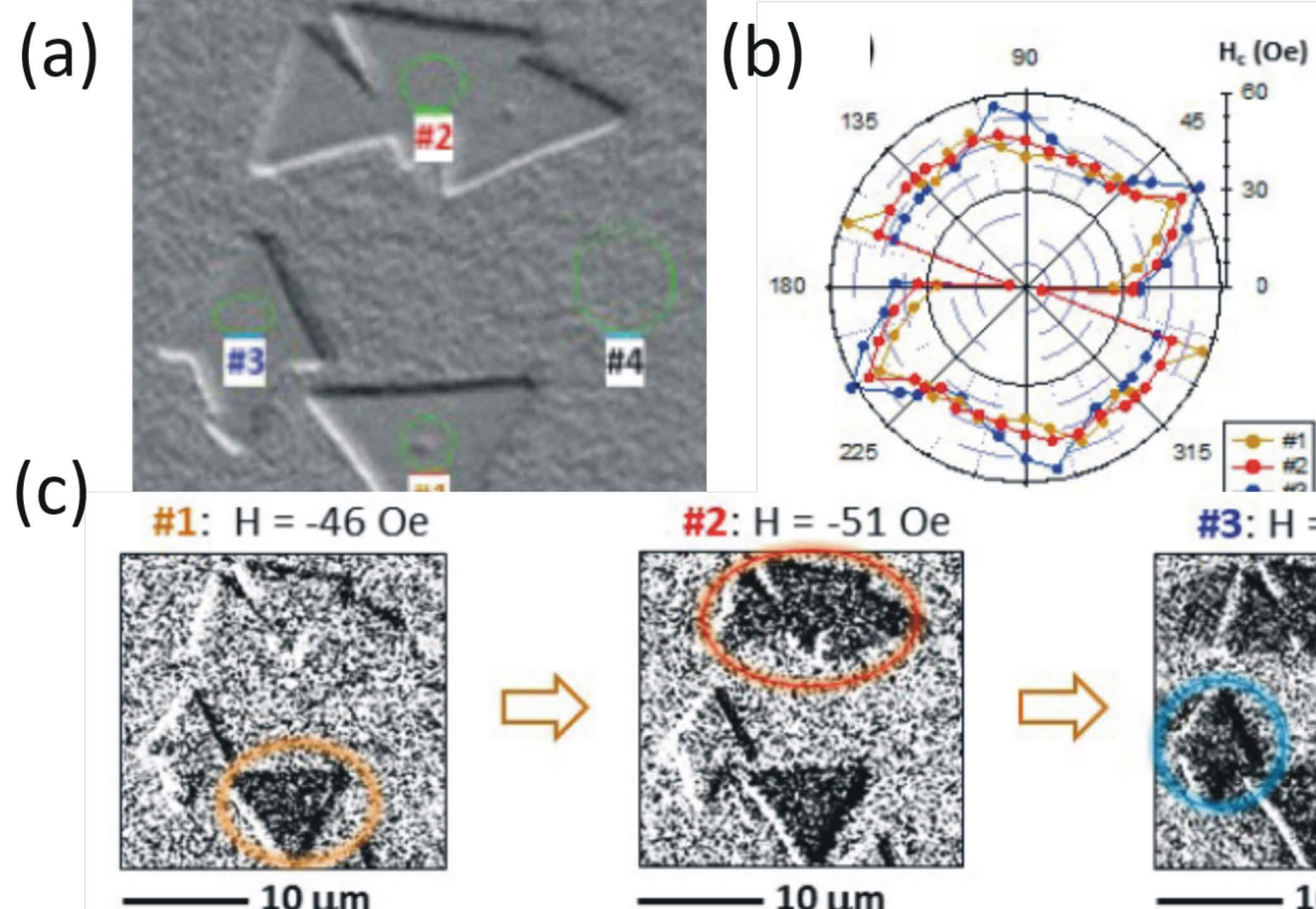
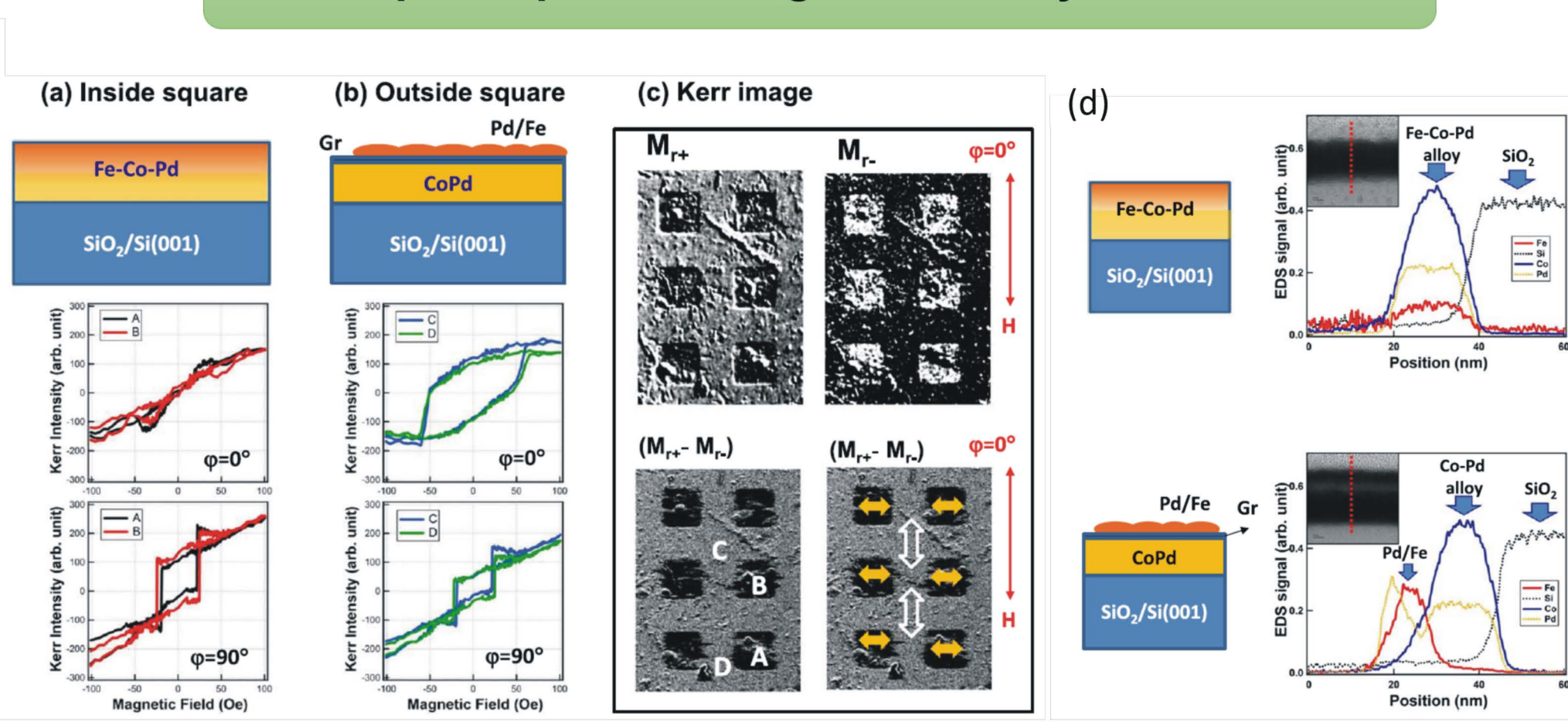


Figure left is shows an  $\psi$ -dependent azimuthal angle related to in-plane magnetic behaviour of the HT-grown 6-nm CoPd/MoS<sub>2</sub> flakes. As indicated in the optical image of Fig. (a), three CoPd/MoS<sub>2</sub> flakes (#1–#3) and CoPd/SiO<sub>2</sub> (#4) were selected for analysis. Fig. (b) shows the magnetic hysteresis loops measured at  $\psi = 90^\circ$  from the four individual areas #1–#4. In Fig. (c), a series of Kerr images recorded at sequential magnetic field exhibit the magnetic switching sequence of the CoPd/MoS<sub>2</sub> flakes.

Figure right is shows the azimuthal angle ( $\varphi$ )-dependent magnetic properties of 2nm Pd/7nm Co/MoS<sub>2</sub> were analyzed. Fig. (e) illustrates the polar plot of the magnetic coercivity ( $H_c$ ) as a function of  $\varphi$ . In Fig.(f), The magnetic domain reversal at 0.9  $H_c$  and  $H_c$  were observed using the magneto-optical Kerr microscope to determine the physical origin of the  $H_c$  change.

##### Graphene protection against interlayer diffusion



Magneto-optical Kerr hysteresis loops measured from (a) Pd/Fe/CoPd and (b) Pd/Fe/Gr/CoPd areas of the annealed sample. The measurements were performed with an in-plane magnetic at azimuthal angles  $\varphi=0^\circ$  and  $90^\circ$ , respectively. (c) Kerr remanence images of the annealed Pd/Fe/patterned-Gr/CoPd sample at  $\varphi=0^\circ$ .  $M_r^+$  and  $M_r^-$  are the remanent states after magnetic saturation in the positive and negative directions, respectively. The red arrows indicate the direction of the magnetic field  $H_c$ . The magnetization directions of the individual areas are indicated in the ( $M_r^+ - M_r^-$ ) images in the lower panel.

(d) EDS cross-sectional depth profiles and elemental mapping for Pd/Fe/CoPd and Pd/Fe/Gr/CoPd areas annealed at 300 °C.



財團法人  
中技社  
CTCI FOUNDATION